

Biomass Valorization

Controlling Reaction Routes in Noble-Metal-Catalyzed Conversion of Aryl Ethers

Julian Schmid[†], Meng Wang[†], Oliver Y. Gutiérrez,^{*} R. Morris Bullock, Donald M. Camaioni, and Johannes A. Lercher^{*}

Abstract: Hydrogenolysis and hydrolysis of aryl ethers in the liquid phase are important reactions for accessing functionalized cyclic compounds from renewable feedstocks. On supported noble metals, hydrogenolysis is initiated by a hydrogen addition to the aromatic ring followed by C–O bond cleavage. In water, hydrolysis and hydrogenolysis proceed by partial hydrogenation of the aromatic ring prior to water or hydrogen insertion. The mechanisms are common for the studied metals, but the selectivity to hydrogenolysis increases in the order Pd < Rh < Ir < Ru ≈ Pt in decalin and water; the inverse was observed for the selectivity to hydrolysis in water. Hydrogenolysis selectivity correlates with the Gibbs free energy of hydrogen adsorption. Hydrogenolysis has the highest standard free energy of activation and a weak dependence on H₂ pressure, thus, the selectivity to hydrogenolysis is maximized by increasing temperature and decreasing H₂ pressure. Selectivity to C–O bond cleavage reaches >95 % in water and alkaline conditions.

Selective cleavage of C–O bonds in aryl ethers is one of the central steps for the valorization of lignocellulosic biomass. The high dissociation energies of C–O bonds and the harsh conditions needed to convert biogenic molecules make the control of reaction pathways challenging.^[1–3] Efforts to address this challenge have focused on studying organic transformations on a wide range of heterogeneous metal,^[4–13] acid,^[14–16] and multi-functional^[17,18] catalysts under a variety

of reaction conditions. Obtaining detailed mechanistic insight, especially regarding the impact of the reaction environment, would foster significant advances in the design of selective catalysts that allow lower reaction temperatures.

Mechanistic studies have focused on the conversion of lignin model compounds (i.e., ethers with α -O-4, β -O-4 and 4-O-5 linkages).^[7,9] In water and alcohols (R–OH), for instance, reductive solvolysis dominates, wherein an aryl ether (Ph–O–R') produces enol ether intermediates (cyclohexene–O–R'), which rapidly add a solvent molecule (Scheme 1). The resulting hemiacetal/acetal eliminates R–OH to form cyclohexanone/cyclohexene–O–R. Pd is remarkably selective for this route.^[10,11,13] Likewise, the hydrogenolytic C–O bond cleavage of aryl ethers on Ni is initiated by one hydrogen addition to the aromatic ring (Scheme 1).^[19]

Seeking a general description of the reaction routes and mechanisms across different metals and a variety of chemical environments, we compare here the reductive conversion of diphenyl ether (Ph₂O) on Ru, Rh, Pd, Ir, and Pt in water and decalin. The selection of Ph₂O allows the study of hydrogenolysis, (reductive) hydrolysis, and hydrogenation (saturation of the aromatic rings without changes in the molecular back-bone).^[10,11,19] We discuss the main reaction mechanisms along these routes and their dependence on reaction parameters. Based on this understanding, we show general strategies to manipulate the reaction network towards higher selectivity for C–O bond cleavage.

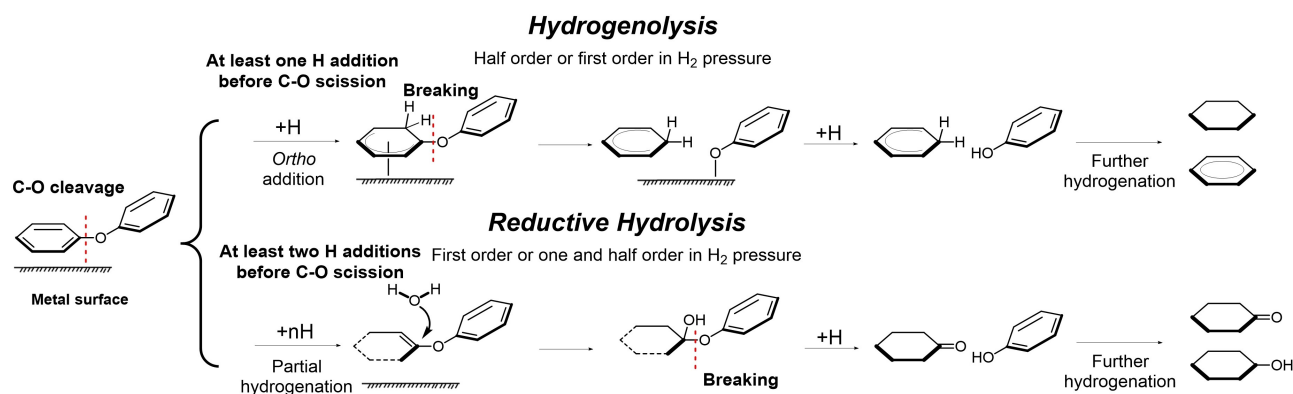
We first consider the reaction mechanisms for the three reaction pathways. The reaction order in H₂ was ≈ 1 for hydrogenation of Ph₂O to cyclohexyl phenyl ether (CyOPh) as the primary product on Rh, Pd, Pt, and Ir (Figure 1A). Only on Ru was the reaction order 1.5 in H₂ (Figure 1A). Assuming that H₂ is dissociatively adsorbed on the metal, these reaction orders indicate that the second hydrogen addition (or the third addition on Ru) to the aromatic ring of Ph₂O is the rate-determining step within a Langmuir–Hinshelwood (L–H) formalism.^[20] The reaction orders in H₂ for the hydrogenolysis pathway were ≈ 0.5 on Rh, Pd, and Pt and ≈ 1 on Ru and Ir (Figure 1B). Our kinetic analysis for the reactions on Rh, Pd, and Pt, indicated that this reaction order suggests one quasi-equilibrated hydrogen addition step prior to C–O bond cleavage as the rate determining step (see the details in Section 3 Supporting Information, Figure S1 and S2 and Table S1). For Ru and Ir, the reaction order indicates that two quasi-equilibrated hydrogen additions occur prior to the C–O bond cleavage in Ph₂O (Section 3 Supporting Information). On the other

[*] J. Schmid,[†] Dr. M. Wang,[†] Dr. O. Y. Gutiérrez, Dr. R. M. Bullock, Dr. D. M. Camaioni, Prof. Dr. J. A. Lercher
 Institute for Integrated Catalysis, Pacific Northwest National Laboratory (PNNL), P.O. Box 999, Richland, WA 99352 (USA)
 E-mail: oliver.gutierrez@pnnl.gov
 johannes.lercher@pnnl.gov

Prof. Dr. J. A. Lercher
 Department of Chemistry and Catalysis Research Institute, Technische Universität München
 Lichtenbergstrasse 4, 85748 Garching (Germany)

[†] These authors contributed equally to this work.

© 2022 The Authors. Angewandte Chemie International Edition published by Wiley-VCH GmbH. This is an open access article under the terms of the Creative Commons Attribution Non-Commercial NoDerivs License, which permits use and distribution in any medium, provided the original work is properly cited, the use is non-commercial and no modifications or adaptations are made.



Scheme 1. Mechanisms of Ni-catalyzed hydrogenolysis and Pd-catalyzed reductive hydrolysis of diphenyl ether.^[11,19]

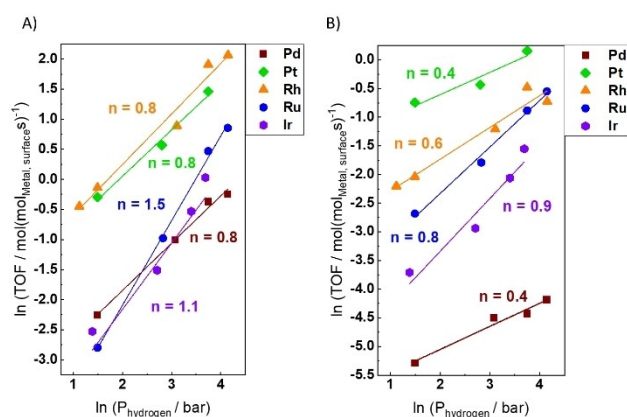


Figure 1. Reaction orders in H₂ pressure for hydrogenation (A) and hydrogenolysis (B) of diphenyl ether on metal catalysts in decalin. Reaction conditions: 5 wt% Metal/C, 10 mmol ether, 40 mL decalin, 150 °C, stirring at 700 rpm. H₂ pressure varies from 4 to 65 bar at room temperature. TOFs were calculated at <20% conversion.

hand, we did not observe an appreciable isotope effect (Table S2). Thus, non-assisted C–O bond cleavage, following the first (or the second) H addition, is likely to be rate determining step in these conditions. This contrasts the mechanism of hydrogenolysis on Ni, where both the C–O bond cleavage and the H addition steps are kinetically relevant.^[19]

Hydrolysis of Ph₂O, which occurs only in water, showed reaction orders of 1–1.5 in H₂. These reaction orders, being nearly identical to those of hydrogenation, and the similar selectivity trends in the two routes (i.e., Pt ≈ Ru < Ir < Rh < Pd) suggest that the aromatic ring is partially hydrogenated prior to the hydrolytic C–O bond cleavage. Thus, this cleavage is a reductive hydrolysis that occurs in parallel to hydrogenation. In line with this conclusion, the sum of selectivities to hydrogenation and hydrolysis measured in water equals the selectivity to hydrogenation observed in decalin (Table 1), where hydrolysis does not occur.

Overall, the similar reaction orders in H₂ and the similar selectivity trends indicate that the reaction mechanisms are similar across the studied metals with variations in the number of quasi-equilibrated hydrogen additions to the

aromatic ring prior to the rate-determining step. This difference causes higher H₂ dependence of the conversion pathways on Ru and Ir. The reaction mechanism for hydrolysis is consistent with that illustrated in Scheme 1. We observe the same dependence of the reaction rates on H₂ for the hydrogenolysis and the hydrogenation route in water and in decalin (Figure 1 and Figure S3). Additionally, selectivity toward the hydrogenolysis route was not influenced by the solvent. This observation applies as well for reactions performed on Pd/C in a selection of alcohols as shown in Table S3.^[10] In contrast, the selectivity to hydrogenation and solvolysis changes significantly. Water promotes high selectivity to solvolysis, which decreases as the size of the alkyl group of the alcohol increases; that is, water > methanol > ethanol > propanol. Decalin, expectedly, did not show reactivity.

On the other hand, the sum of selectivity for hydrogenation and hydrolysis in water equals the selectivity for hydrogenation in decalin on all tested metals. Thus, we conclude that the solvent does not change the mechanisms of Ph₂O hydrogenation and hydrogenolysis, although the rates for both routes are generally higher in water than in decalin. We derived rate equations for hydrogenolysis and hydrogenation pathway and used them for fitting the kinetic data from reactions on different metals in decalin (Section 3, Supporting Information). The fitting agreed well with one (Rh, Pd, and Pt) or two (Ru and Ir) quasi-equilibrated hydrogenation steps to the C–O bond cleavage as a rate-determining step. Similarly, for hydrogenation, there are more equilibrated hydrogen addition steps on Ru (three) than on Rh, Pd, Ir, and Pt (two), prior to the limiting step.

Having discussed the reaction mechanisms across the studied solvents and metals, we turn to their overall catalytic properties. The intrinsic activity (i.e., TOFs) of the studied metals increased in the order Pd < Ir < Ru < Pt < Rh for both solvents at 150 °C. The difference in activities at this temperature were within an order of magnitude, Rh being 10 × more active than Pd (Table 1). The same general trend was observed in the studied temperature range (Table S4–S8). Generally, hydrogenation dominated in most of the reaction conditions studied. The selectivity to hydrogenolysis increased in the order Pd < Rh < Ir < Ru ≈ Pt while the reverse

Table 1: Reactions of diphenyl ether on different metal catalysts in decalin or water under H₂.^[a]

Metal	$E_{\text{ads}}(\text{H}_2)^{[b]}$ [kJ mol ⁻¹]	Decalin			Water			
		TOF ^[c] [s ⁻¹]	Reaction routes selectivity (TOF) ^[d]		TOF ^[c] [s ⁻¹]	Reaction routes selectivity (TOF) ^[d]		
			Hydrogenolysis	Hydrogenation		Hydrogenolysis	Hydrogenation	Hydrolysis
Ru	71	2.0	21% (0.4)	79% (1.4)	5.7	20% (1.1)	69% (3.9)	11% (0.6)
Rh	100	7.4	9% (0.7)	91% (6.7)	29	5% (1.45)	82% (24)	13% (3.7)
Pd	97	0.70	2% (0.01)	98% (0.7)	0.64	2% (0.013)	81% (0.5)	17% (0.1)
Ir	96	1.2	17% (0.2)	83% (1.0)	2.3	13% (0.30)	84% (1.9)	3% (0.07)
Pt	67	5.5	20% (1.1)	80% (4.4)	12	22% (2.55)	67% (7.8)	11% (1.3)

[a] Reaction conditions: diphenyl ether (1.70 g), 5 wt% (10.0 mg or 1.0 mg) Metal/C, 80 mL water or 40 mL decalin, 150 °C, 58 bar of H₂ (40 bar at room temperature), stirring at 700 rpm. [b] Heat of adsorption of H₂ on metal surface.^[21–24] [c] TOF = turnover frequency. Calculated at <20% conversion. [d] Hydrogenolysis = 2 × (cyclohexane + benzene); hydrolysis = (phenol + cyclohexanone + cyclohexanol) – hydrogenolysis; hydrogenation = (phenyl cyclohexyl ether + dicyclohexyl ether).

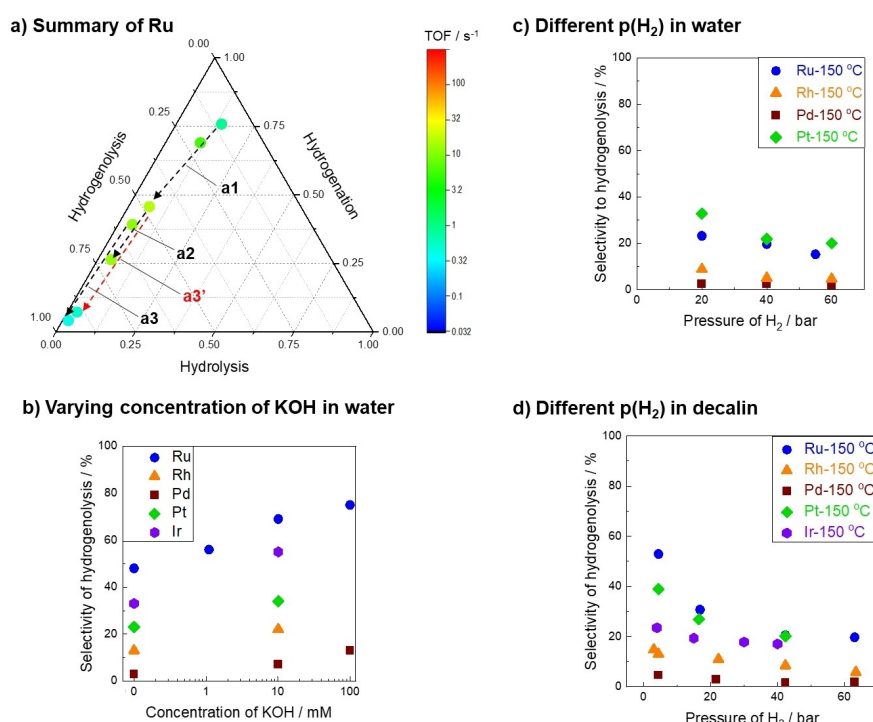


Figure 2. a) Changes in selectivity on Ru in water following different strategies, a1) reaction temperature increased from 100 to 200 °C at 40 bar H₂ pressure; a2) Addition of KOH up to 10 mM at 200 °C and 40 bar H₂; a3) Lowering the H₂ pressure from 40 bar to 4 bar at 200 °C in 10 mM KOH solution. a3') Lowering the the H₂ pressure from 40 to 4 bar at 200 °C (b) Selectivity to hydrogenolysis with varying concentrations of KOH solution at 200 °C and 40 bar H₂. c) Selectivities to hydrogenolysis under varying H₂ pressure in water. d) Selectivities to hydrogenolysis under varying H₂ pressure in decalin.

trend was observed for reductive hydrolysis in water. This is in line with the outstanding selectivity of Pd to catalyze hydrolysis.^[11]

Varying the reaction parameters, we identified clear trends of selectivity changes for Ph₂O conversion (Table S4–S8, Figure 2a and Figure S4). As we have reported on Pd and Ni,^[11,19] the C–O cleavage reactions have higher energies of activation than hydrogenation. For instance, 85 kJ mol⁻¹ for hydrogenolysis compared to 62 kJ mol⁻¹ and 55 kJ mol⁻¹ for hydrolysis and hydrogenation, respectively, on Rh (Table S9 and S10). Thus, higher selectivity to the cleavage reactions was achieved at higher temperatures. Increasing

the H₂ pressure increases the rates of all pathways. The H₂ dependence, however, was the lowest for hydrogenolysis compared to the other two pathways on all tested metals leading to higher selectivity toward C–O bond cleavage at lower pressures (Figure 1 and Figure S3). To probe the generality of these conclusions for a larger variety of materials, we also tested a larger set of commercial and house-made catalysts. The trends obtained with different sets of catalysts were identical; the differences in rates are attributed to differences in the particle size of the supported metal (Figure S5 and Table S11). Interestingly, the selectivity of each catalyst did not change, which we attribute to the

absence of changes in the electronic properties of the supported particles (i.e., a subjacent reason of possible differences in adsorption properties) within the studied dispersion range.

The conversion of Ph₂O in water opens hydrolysis as additional C–O bond cleavage route. Water is the most reactive solvent toward insertion to the enol ether intermediate in this path.^[10,11] Moreover, the aqueous medium offers the opportunity of varying the concentration of hydronium ions. We observed that the rates of hydrogenation and hydrogenolysis decreased with the addition of a base, with a net effect of increasing the selectivity to hydrogenolysis (Table S4–S8). This suggests that alkaline conditions increase the hydrogen binding strength, which in turn decreases the rate constant of hydrogen addition.^[25,26] As more hydrogen atoms are involved in hydrogenation than in hydrogenolysis this effect is stronger for the former and favors so hydrogenolysis.

Selectivity toward the different pathways depends strongly on reaction conditions, as illustrated by specific changes in the selectivity in water. Setting our reference conditions at 100 °C, and high pressures of H₂ (40–60 bar) (Figure 2a, Figure S4), the conversion is dominated by the hydrogenation pathway. The selectivity to C–O bond cleavage (hydrogenolysis and hydrolysis) increased on all metals by increasing temperature (up to 200 °C) and decreasing H₂ pressure (to 4 bar). The selectivity to hydrogenolysis on Ru, for instance, changed from 10% at the reference conditions to 47% with increasing temperature and to 90% when reducing the H₂ pressure to 4 bar. When increasing concentrations of KOH (1, 10, and 100 mM of KOH solutions) were used in the reaction mixture at 200 °C and 40 bar, the selectivity to hydrogenolysis increased to 5%, 69%, and 75%, respectively (Figure 2b and c). Performing the reaction at 200 °C, 4 bar of H₂ pressure, in an aqueous solution of 10 mM KOH, we were able to achieve 94% selectivity toward hydrogenolysis products.

Similarly, the selectivity to hydrogenolysis in decalin can be tuned by increasing the reaction temperature from 100 °C to 150 °C (the selectivity changes from 15% to 21%) and decreasing the H₂ pressure from 60 to 4 bar (selectivity changes from 21% to 53%, Figure 2d).

High selectivity to hydrogenation was achieved when the reaction conditions were shifted toward low temperature and high H₂ pressure. As the reaction mechanisms are similar on all metals, the reaction conditions have the same effect on selectivity as shown in the Supporting Information (Figure S4 for Rh, Pd, Ir and Pt and the corresponding data is listed in Tables S4–S8).

An inverse relationship between the selectivity for hydrogenolysis in decalin and the Gibbs free energies of H₂ adsorption on the different metals has been observed (Figure 3 and Table S14 for the explored pressure range). Thus, we attribute the selectivity difference between the two competitive reaction pathways—hydrogenolysis and hydrogenation—to the coverage of the metals with H₂. Higher coverage of H₂ on the respective metal surface favors hydrogenation, while lower coverage increases the probability for the hydrogenolysis route. Note that the overall

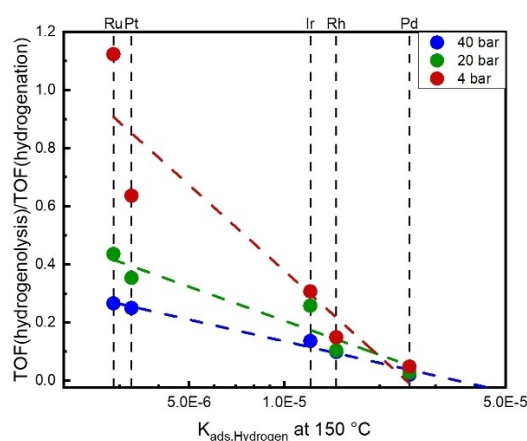


Figure 3. Correlation between the ratio of the rates of hydrogenolysis and hydrogenation (40, 20 and 4 bar) and the equilibrium constants for H₂ adsorption at 150 °C for different metals. The data at 40 and 4 bar are direct measurements, the 20 bar points are extrapolations from experimental data.

reactivity trends do not scale with the hydrogen coverage or with the apparent activation energies (Tables S1, S9, and S10). Thus, we surmise that a combination of pre-exponential factor and activation barrier (entropy and enthalpy of transition state) determines the reactivity trends.

In conclusion, we found that partial hydrogenation of the aromatic rings is a key step in hydrogenolysis and hydrolysis of the C–O bond in diphenyl ether on Ru, Rh, Pd, Ir and Pt. This partial hydrogenation breaks the aromaticity of the adsorbed molecule, facilitating the C–O bond cleavage. Despite differences in the number of equilibrated hydrogen additions prior to the rate-determining step, the reaction mechanisms of the conversion pathways are invariable over different metals in water and decalin. The descriptor for the selectivity of hydrogenation and hydrogenolysis is the adsorption energy of H₂ on the different metals, i.e., relatively weak interactions (and concomitant low hydrogen coverages) favor the C–O bond cleavage. The commonly high hydrogenation selectivity of the Pt-group metals was shifted to C–O bond cleavage (i.e., from >69% hydrogenation to >95% hydrogenolysis in the case of Ru) by fine-tuning the reaction conditions. These findings serve as guidelines to steer selectivity in complex environments and are the basis for advancing understanding of the consequences of solvent and catalyst compositions on metal-catalyzed cleavage of aromatic ether bonds.

Supporting Information: Experimental methods, additional information, Figures S1–S15 and Tables S1–S14.

Acknowledgements

This work was supported by the U.S. Department of Energy, Office of Science, Office of Basic Energy Sciences, Division of Chemical Sciences, Geosciences, and Biosciences (FWP 47319). Open Access funding enabled and organized by Projekt DEAL.

Conflict of Interest

The authors declare no conflict of interest.

Data Availability Statement

The data that support the findings of this study are available from the corresponding author upon reasonable request.

Keywords: Biomass Conversion · C–O Bond Cleavage · Hydrogen · Noble-Metal Catalysts · Solvent Effects

-
- [1] M. Zaheer, R. Kempe, *ACS Catal.* **2015**, *5*, 1675–1684.
- [2] J. Zakzeski, P. C. A. Bruijninx, A. L. Jongerius, B. M. Weckhuysen, *Chem. Rev.* **2010**, *110*, 3552–3599.
- [3] P. J. Deuss, K. Barta, *Coord. Chem. Rev.* **2016**, *306*, 510–532.
- [4] V. Molinari, G. Clavel, M. Graglia, M. Antonietti, D. Esposito, *ACS Catal.* **2016**, *6*, 1663–1670.
- [5] R. Ma, W. Hao, X. Ma, Y. Tian, Y. Li, *Angew. Chem. Int. Ed.* **2014**, *53*, 7310–7315; *Angew. Chem.* **2014**, *126*, 7438–7443.
- [6] T. Prasomsri, M. Shetty, K. Murugappan, Y. Román, R. Román-Leshkov, *Energy Environ. Sci.* **2014**, *7*, 2660–2669.
- [7] J. He, C. Zhao, J. A. Lercher, *J. Am. Chem. Soc.* **2012**, *134*, 20768–20775.
- [8] J. Lu, M. Wang, X. Zhang, A. Heyden, F. Wang, *ACS Catal.* **2016**, *6*, 5589–5598.
- [9] J. Zhang, J. Teo, X. Chen, H. Asakura, T. Tanaka, K. Teramura, N. Yan, *ACS Catal.* **2014**, *4*, 1574–1583.
- [10] M. Wang, O. Y. Gutiérrez, D. M. Camaioni, J. A. Lercher, *Angew. Chem. Int. Ed.* **2018**, *57*, 3747–3751; *Angew. Chem.* **2018**, *130*, 3809–3813.
- [11] M. Wang, H. Shi, D. M. Camaioni, J. A. Lercher, *Angew. Chem. Int. Ed.* **2017**, *56*, 2110–2114; *Angew. Chem.* **2017**, *129*, 2142–2146.
- [12] Q. Xia, Z. Chen, Y. Shao, X. Gong, H. Wang, X. Liu, S. F. Parker, X. Han, S. Yang, Y. Wang, *Nat. Commun.* **2016**, *7*, 11162.
- [13] Q. Meng, M. Hou, H. Liu, J. Song, B. Han, *Nat. Commun.* **2017**, *8*, 14190.
- [14] A. K. Deepa, P. L. Dhepe, *ACS Catal.* **2014**, *5*, 365–379.
- [15] M. Siskin, A. R. Katritzky, M. Balasubramanian, *Energy Fuels* **1991**, *5*, 770–771.
- [16] P. J. Deuss, M. Scott, F. Tran, N. J. Westwood, J. G. De Vries, K. Barta, *J. Am. Chem. Soc.* **2015**, *137*, 7456–7467.
- [17] X. Huang, C. Atay, T. Tamás, I. K. Korányi, M. D. Boot, E. J. M. Hensen, *ACS Catal.* **2015**, *5*, 7359–7370.
- [18] X. Wang, R. Rinaldi, *Catal. Today* **2016**, *269*, 48–55.
- [19] M. Wang, Y. Zhao, D. Mei, R. M. Bullock, O. Y. Gutiérrez, D. M. Camaioni, J. A. Lercher, *Angew. Chem. Int. Ed.* **2020**, *59*, 1445–1449; *Angew. Chem.* **2020**, *132*, 1461–1465.
- [20] Z. Zhao, R. Bababrik, W. Xue, Y. Li, N. M. Briggs, D.-T. Nguyen, U. Nguyen, S. P. Crossley, S. Wang, B. Wang, D. E. Resasco, *Nat. Catal.* **2019**, *2*, 431–436.
- [21] I. Toyoshima, G. A. Somorjai, *Catal. Rev.* **1979**, *19*, 105–159.
- [22] C. H. Bartholomew in *Catalysis, Vol. 11* (Eds.: J. J. Spivey, S. K. Agarwal), The Royal Society Of Chemistry, Cambridge, **1994**.
- [23] Z. Paál, P. G. Menon, *Catal. Rev.* **1983**, *25*, 229–324.
- [24] K. R. Christmann in *Hydrogen Effects in Catalysis: Fundamentals and Practical Applications* (Eds.: Z. Paál, P. G. Menon), Marcel Dekker, New York, **1988**.
- [25] N. Singh, M.-S. Lee, S. A. Akhade, G. Cheng, D. M. Camaioni, O. Y. Gutiérrez, V.-A. Glezakou, R. Rousseau, J. A. Lercher, C. T. Campbell, *ACS Catal.* **2019**, *9*, 1120–1128.
- [26] G. Cheng, A. Jentys, O. Y. Gutiérrez, Y. Liu, Y.-H. Chin, J. A. Lercher, *Nat. Catal.* **2021**, *4*, 976–985.

Manuscript received: February 28, 2022

Accepted manuscript online: April 28, 2022

Version of record online: June 14, 2022